Shared Control Between Human and Machine: Haptic Display of Automation During Manual Control of Vehicle Heading

Paul Griffiths R. Brent Gillespie
Department of Mechanical Engineering University of Michigan, Ann Arbor, MI 48109, USA
paulgrif, brentg@umich.edu

Abstract

In this paper, a paradigm for shared control is described in which a machine's manual control interface is motorized to allow a human and an automatic controller to simultaneously exert control. The manual interface becomes a haptic display, relaying information to the human about the intentions of the automatic controller while retaining its role as a manual control interface. The human may express his control intentions in a way that either overrides the automation or conforms to it. The automatic controller, by design, aims to create images in the mind of the human of fixtures in the shared workspace that can be incorporated into efficient task completion strategies. The fixtures are animated under the guidance of an algorithm designed to automate part of the human/machine task. Results are presented from 2 experiments in which 11 subjects completed a path following task using a motorized steering wheel on a fixed-base driving simulator. These results indicate that the haptic assist through the steering wheel improves lane keeping by at least 30% reduces visual demand by 29% ($p<0.0001$) and improves reaction time by 18 ms ($p=0.0009$).

1. Introduction

When controlling a machine through a manual control interface, one has the opportunity to simultaneously apply control action and monitor response. Information may flow in both directions across the mechanical contact between human and machine. In this paper, we present a scheme for coordinating machine control between a human and an embedded controller that uses the response information channel to facilitate that coordination. The manual control interface is motorized for application of the embedded controller's control action, but also for display of that action to the cooperating human. By motorizing the manual control interface, it becomes a haptic interface, advertising the control actions of the embedded controller. The embedded controller is placed in mechanical parallel with the human, where the two then share control over the machine using the language of mechanical interaction. With access to the action of the automation through haptics, the human can efficiently form mental models of the automation system. The human can retain authority but also turn his attention to other tasks without incurring a performance loss in the semi-automated task. We envision this shared control scheme for various machines that feature embedded controllers, yet do not function autonomously—machines whose control requires the abilities of the human to accommodate and recover from unexpected operating conditions, to build predictive mental models, and to process and parse rich sensory information. One such machine is the automobile.

Various schemes have been proposed by which a human and automatic controller may share control, including supervisory control and human-centered automation [1]. Sharing control, however, always presents special challenges. The division of responsibilities must be carefully and continually negotiated. Sensed information, control plans, and even models by which behavior is predicted must be communicated between the two cooperating controllers. We propose that the paradigm for control sharing described in this paper is much like the paradigm used between two humans who work together manually on the same task. Even while exerting control, one of the humans may monitor the actions of the other while imposing his own control. He may even impose his control using a certain impedance that expresses his confidence in the appropriateness of this control intentions.

In this paper, we study shared control of automobile steering. The steering wheel is both grasped by the driver and motorized for automatic control. The motion of the steering wheel is then a response to the sum of forces acting from the human grasp, from the automatic control motor, and from the steering linkage. The key to communication through the steering wheel is that even while applying a torque, the human can monitor the steering wheel motion. Alternatively, if the human is considered to impose motion on the steering wheel, he can simultaneously monitor interaction torque. With an internal model of the steering linkage

and vehicle behavior (perhaps informed by other sensory inputs), the human may differentiate the control actions being expressed by the automatic controller from the response of the vehicle and steering linkage. Negotiation of authority is also possible: upon sensing the intentions of the automatic controller through his grip on the steering wheel, he can judge them either reasonable or inappropriate, and can choose to yield to those intentions or to override them.

To allow its authority to be over-ridden by the human, the embedded controller exerts it control with a certain finite impedance. That impedance is defined using proportional control, which might also be interpreted as a virtual fixture [2] that is defined not just in space but also in time. In effect, a potential well is created, but a potential well that moves with the control signal generated by the embedded controller. Virtual fixtures that similarly were functions of time were used in [3], where fixtures were turned on and off based on recognized operator motions. Our shared-control technique adds an animated virtual fixture or perceptual overlay on the road by actuating the steering system of a car. The human, by feeling the actions of the controller under his grip on the interface, will project images into the task space, such as a virtual rut in the road. Given prior experience with similar objects in the physical environment, such virtual fixtures should be easy to recognize and negotiate.

Driving is certainly an application where humans are reluctant to give up autonomy, yet the introduction of automatic control features could significantly increase vehicle and highway safety and efficiency. Increasing demands are being made on drivers' attention, which further motivates the introduction of automatic control to reduce drivers' mental workload. With the introduction of steer-by-wire systems in future vehicles, the steering wheel will already be motorized for haptic display of reaction torques from the road, so the addition of haptic display of an automated steering system requires no additional actuator. Other technologies to support automated vehicle control are under development, including Global Positioning Systems (GPS), radar systems, imaging systems, and magnetic highway markers. Another, perhaps more immediately viable application for shared control of vehicle heading is in agricultural vehicles, where GPS-guided tractors are already commercially available [4] [5].

For automobile control in both the longitudinal and lateral directions, various forms of driver assist are available or under development, and some of these utilize haptic display through a motorized steering wheel [6] [7]. In most conceptions of driver assist, information or warning is offered to the driver, but an alternative strategy suggests evasive action, while requiring the driver to take that action. In our shared control scheme, the assist actually intervenes in the control loop. The driver may yield to the assist while monitoring its action.

We present two experiments designed to demonstrate our conception of shared control using a motorized manual control interface. Naturally, an expected outcome is improved performance on the semi-automated task. However, there are other expected benefits. The first experiment is aimed at quantifying the benefits in reduced perceptual demand associated with a primary task (in this case visual demand). In the second experiment, we investigate a hypothesized reduction in cognitive load or a freeing of attention (as reflected by improved performance on a secondary task). The primary task in both experiments also includes a challenge not addressed by the automatic controller, which becomes a means for prompting negotiations between the human and automation, and a basis for requiring and measuring maintained vigilance by the human. A possible cost to our shared control approach is increased physical workload, because to override the automatic controller, the human must impose his control efforts with greater force. We do not evaluate the increased physical workload, but we scale the actions of the automatic controller such that the increased physical workload is relatively small and not objectionable.

In section 2.5 we describe the driving simulator and shared steering controller used for our experiments. We also present a simplified human driver model that features haptic feedback and use this model to describe the exchange of information over both haptic and visual channels with the simulator and automatic steering controller. In section 3 the first experiment testing reduced visual demand is described and its results presented and discussed. In section 4 the experiment on reduced mental workload is described and its results presented and discussed.

2. Methods

The driving simulator used in the experiments uses a 17-inch computer monitor for visual display and a motorized steering wheel for haptic interface. It lacks motion display and audio display. The computational portion of the simulator is based on a simple kinematic model of a car and an idealized steering linkage without dynamics. The car runs at a constant forward speed and thus lacks longitudinal dynamics and foot pedals. The car may be steered through a pre-set driving course of straight and curved segments. The automatic controller runs on the same computational hardware as the driving simulator. In this section, we describe the driving simulator, the automatic controller, and the motorized steering wheel in detail. We also present a model of a driver to highlight its coupling to the motorized steering wheel and simulated car and steering controller. The driver model features explicit haptic feedback, showing how the driver can simultaneously express his intentions and monitor the actions of the steering controller and response of the vehicle, both haptically and visually. We assemble the driv-

ing simulator and driver model in a block diagram to highlight the interactions, especially the haptic (mechanical) interactions between driver, vehicle simulator, and automatic controller. Additional detail regarding the synthesized visual feedback and support for data recording and experimental protocol, including secondary task presentation and measurements, will be described in section 2.5.

2.1. Vehicle Model

Figure 1 shows a top view of a vehicle whose configuration in the X-Y plane may be specified using the coordinates (x, y) of the vehicle center-point C and the angle ψ between the vehicle centerline and the X-axis. The vehicle has two rear wheels on axles fixed perpendicular to the centerline and two front wheels on axles that may be oriented through a steering linkage. The common heading angle of both front wheels relative to the centerline of the vehicle is δ.

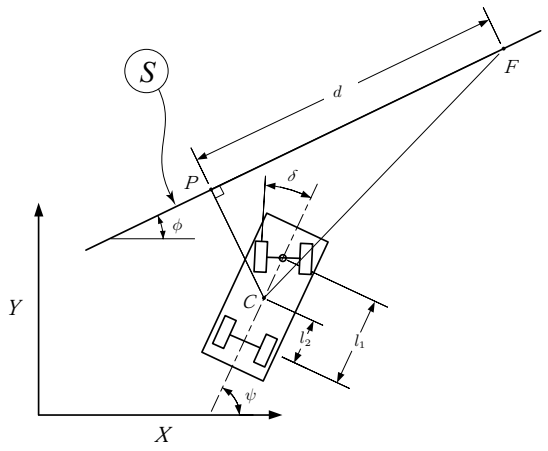

Figure 1. A bicycle model vehicle is shown with respect to the global coordinate frame X-Y and in relation to the roadway S.

Assuming no slip between the tires and the road, the kinematics of the vehicle are given by the bicycle model. Given δ and the speed of the front axle u as inputs, the motion of the vehicle is governed by the following set of differential equations.

$$\dot{x} = -\frac{ul_2}{l_1}\sin\delta\sin\psi + u\cos\delta\cos\psi \quad (1)$$

$$\dot{y} = \frac{ul_2}{l_1}\sin\delta\cos\psi + u\cos\delta\sin\psi \quad (2)$$

$$\dot{\psi} = \frac{u}{l_1}\sin\delta \quad (3)$$

Due to interaction between the front wheels and the road, a so-called self-aligning torque σ_{sa} acts on the steering linkage and tends to drive the steering angle δ to zero.

$$\sigma_{sa} = -A_k\delta \quad (4)$$

Although the proportionality constant A_k is in general a function of the speed u, for our purposes A_k is a constant since the driving simulator uses a constant speed.

2.2. Steering Wheel and Steering Linkage

The steering angle δ is related to the angular displacement of the steering wheel (handwheel) through a steering linkage. We model the steering linkage as an ideal transmission of mechanical advantage R, whose inputs are the angular displacement of the steering wheel θ and the self-aligning torque σ_{sa}. The outputs of the steering linkage are the steering angle δ that drives the kinematic model introduced above and a self-aligning torque τ_{sa} that is imposed on the steering wheel.

$$\begin{aligned} \delta &= R\theta \\ \tau_{sa} &= R\sigma_{sa} \end{aligned} \quad (5)$$

We neglect compliance in the steering linkage and lump inertial and damping effects with the inertia and damping of the steering wheel. We designate θ as a degree of freedom or state variable in the system model so that θ is available through an application of Newton's law if the sum of torques acting on the steering wheel and the inertia J and damping b are known. Parameter J accounts for the inertia of the steering wheel and the equivalent inertia of the steered wheels and steering linkage and b accounts for the damping between the steering wheel, the steering linkage and the vehicle frame.

In our driving simulator, Newton's law is carried out not in simulation, but in mechanical hardware. A physical steering wheel of inertia J twice "integrates" the sum of torques acting on the steering wheel, including any torque applied by a human driver, and any torque applied by a motor coupled to the steering wheel. The torque τ_{sa}, which is reflected from a simulated vehicle, and the torque produced by an automatic steering controller, introduced next, are both applied to the physical steering wheel by a motor.

2.3. Steering Controller

The steering controller imposes a torque τ_c on the steering wheel through a motor that is coupled to the steering wheel with a chain drive. The signal τ_c driving the motor is designed to cause the steering wheel angular displacement θ to follow a desired angle $\theta_d(t)$ through a simple proportional control law:

$$\tau_c = K_a(\theta_d - \theta) \quad (6)$$

where K_a is a gain that may be tuned for performance. The desired steering wheel angle θ_d is computed in turn by a

steering controller that monitors the vehicle coordinates x, y and vehicle heading ψ in relation to a known map of the driving course. To begin, suppose that the road is straight as in Figure 1, which shows the vehicle in proximity to a straight segment S of the road.

A desired front wheel heading angle δ_d is sought that brings the vehicle's trajectory onto S. The point P on S lying closest to C is found by a feedback stabilized closest-point algorithm and the point F lying on S a look-ahead distance d ahead of P is found. Then the angle subtended by the line segment $\overline{CF}$ and the vehicle centerline is the desired heading angle for the front wheels is δ_d for the case of a straight road. The steering wheel desired angle $\theta_d = R\delta_d$, and the angle δ_d is given by:

$$\delta_d = \phi - \psi - \tan^{-1}(e/d) + \delta_o \tag{7}$$

$$e = \overline{PC} \cdot (\sin\phi X - \cos\phi Y) \tag{8}$$

where ϕ_0 is defined below.

In general, the path S is not straight. For any constant curvature κ, an offset steering angle can be found such that the vehicle trajectory has the same curvature as the road. When the vehicle is close to S, applying $R\delta_o$ as an offset to the steering wheel converts a curved centerline S back into a straight segment. Using a small angle approximation, the offset angle δ_o is given by:

$$\delta_o = \kappa L \tag{9}$$

The offset angle δ_0 is applied to produce δ_d for an S of any constant curvature κ. The sign convention of κ is positive for a left curving road.

The trajectory generated by this control law has several attractive properties. The desired steering angle is based on the predictive driver modeling of Hess and Modjtahedzadeh [8]; specifically, it replicates the idea of an "aim-point" ahead of the vehicle on the centerline of the road. If the human driver also follows this model to determine a desired steering angle, the controller will, in some sense, not fight the driver but rather mimic the driver's behavior. Additionally, the trajectory generated by following δ_d has a lateral deviation that is exponentially stable without overshoot for any initial lateral deviation.

2.4. Driver Model with Haptic Feedback

Figure 2 shows a block diagram that links together the system components presented so far (the vehicle kinematics, the steering wheel and steering linkage, and the automatic steering controller) with a model of the driver. The the vehicle kinematics, steering wheel, steering linkage, and steering controller have been fully detailed above, since they make up the driving simulator. We do not attempt to fully model the driver. However, Figure 2 presents a driver model in which haptic feedback is shown explicitly. The driver is modeled as a motion source, using muscle action to produce an angular displacement θ_h of the hands on the steering wheel, measured as rotation about the steering wheel axis. Between the hand that moves with θ_h and the steering wheel that moves with θ is soft tissue, finger pulp and skin, including skin-stretch sensors that are modeled as a linear spring with stiffness K_s. The difference in displacement $\theta_h - \theta$ produces the torque τ_h that acts on the steering wheel, causing it to follow the intentions of the driver. In all, a sum of the three torques τ_h, τ_c, and τ_{sa} act on the steering wheel to produce the displacement θ. With an estimate of the steering wheel dynamics and knowledge, through the skin stretch sensors of the torque τ_h, the driver can monitor the torque τ_c applied by the automatic controller and the self-aligning torque τ_{sa}. The haptic feedback τ_h provides a reading of the actions taken by the automatic controller that shares control over the vehicle.

Also indicated in Figure 2 are the portions of the driving simulator that are rendered in hardware and those that are rendered in software, in simulation. The blocks outlined in a double line represent physical hardware, while the remaining processes are simulated in software. The open arrowheads represent either electrical or neural signals while the filled arrow-heads are mechanical variables. The motor and an accompanying amplifier (including a digital-to-analog converter) are the interface for the computer to the physical hardware while an angular displacement sensor and sampler (including an analog-to-digital converter) is the means for the computer to monitor physical hardware.

From Figure 2 it is apparent that the driver and the controller act in parallel on the steering system. In addition to the haptic feedback signal τ_h, the driver has access to the vehicle configuration variables x, y and ψ and the road geometry through vision. (In an actual vehicle, the vestibular sense also helps in the estimation of the vehicle configuration.) The automated steering controller has access to the vehicle state x, y, and ψ through sensors such as GPS (or in the case of a simulator through shared variables) and it has access to the road geometry either through an internal map or road geometry sensors.

The driver, prompted by the torque $\tau_h = J\ddot{\theta} + b\dot{\theta} - \tau_{sa} - \tau_c$ that he feels through the motorized steering wheel, may imagine that the front tires are rolling along ruts in the road. If the driver has a sufficiently accurate model of τ_{sa} based on θ, and can estimate J and b, then τ_h can be used to estimate τ_c, the action of the automatic steering controller.

2.5. Simulator Environment and Features

The computational hardware supporting the driving simulator included two computers: a PC for graphical display and a Motorola MPC-555 PowerPC-based microcontroller for the real-time simulation of the vehicle model and steering controller. An OpenGL graphics application running on

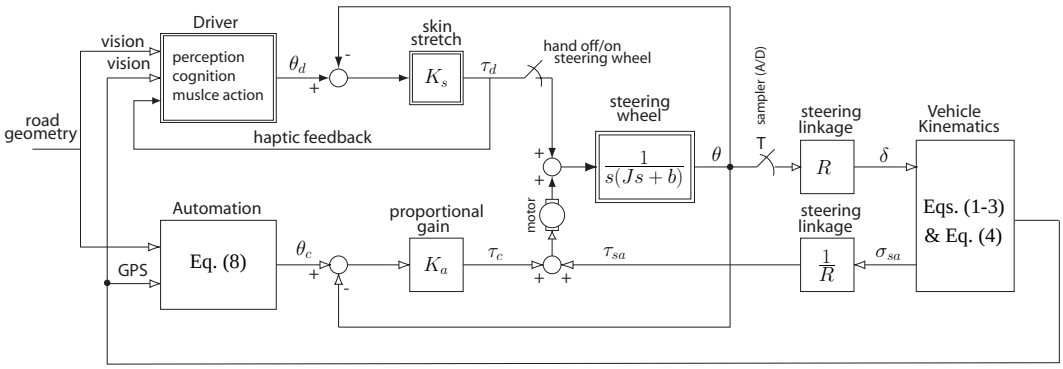

Figure 2. The block diagram shows the general structure of the shared control.

the PC rendered a 3-D animation of the hood of the car and the road. The graphics software received the vehicle state information every 8 ms through a serial communication link to the MPC555-based board. The road was designed to look like a 10 m wide concrete roadway with a solid yellow centerline. A screen-shot from the animation is shown in Figure 3. The road consisted of 16 straight segments and 15 left and right curve segments of constant curvature and varying length. Thirty orange solid cylinders were located in the center of the road along the course to act as obstacles. The separation between cylinders varied according to a uniform random distribution between 20 and 80 meters. Figure 4 shows a top view of the roadway and the obstacles. The roadway length is 1993 m and the vehicle's front axle speed is 7 m/s. Taking into account the acceleration and deceleration at the beginning and end of the course along and the slightly longer distance traversed by the vehicle, the course is driven in just under five minutes.

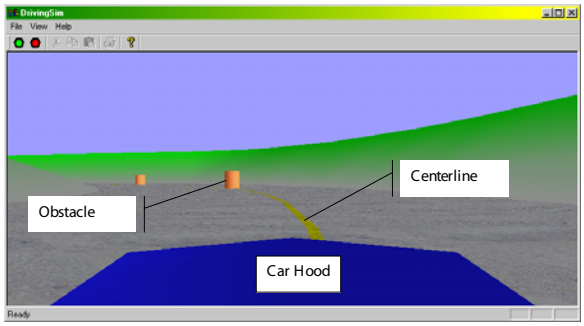

Figure 3. An OpenGL animation of the roadway visible over the hood provided subjects with visual feedback (labels added).

The haptic wheel shown in figure 5 served as the steering wheel interface for the driving simulator. The microcontroller sampled the angular position θ of the wheel and commanded a torque to the wheel's current-controlled motor according to the computed tire self-aligning torque τ_{sa} and the steering assist torque τ_c.

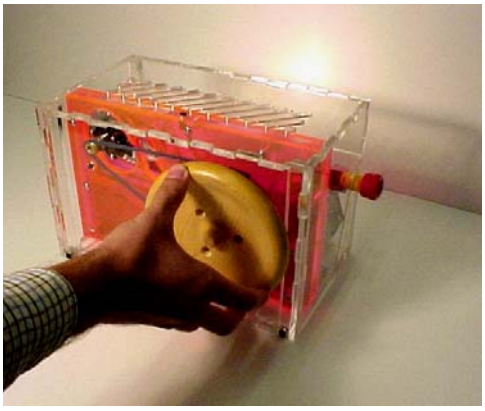

Figure 5. The haptic wheel shown above functioned as a motorized steering wheel.

3. Experiment I

3.1. Protocol

The first experiment was aimed at quantifying the ability of the haptic assist controller to aid subjects in a path following task while reducing demand for visual cues. Some attention to the shared path following task was required of the driver in order to avoid hitting the obstacles in the middle of the road, since the assist controller had no information about the obstacles. The obstacles provided the motivation for keeping the human in the loop.

Eleven participants, 9 male and 2 female between the ages of 20 and 63 were recruited for the study. Subjects were asked if they had good, balanced hearing for spatial location of sounds. Each subject provided informed consent in

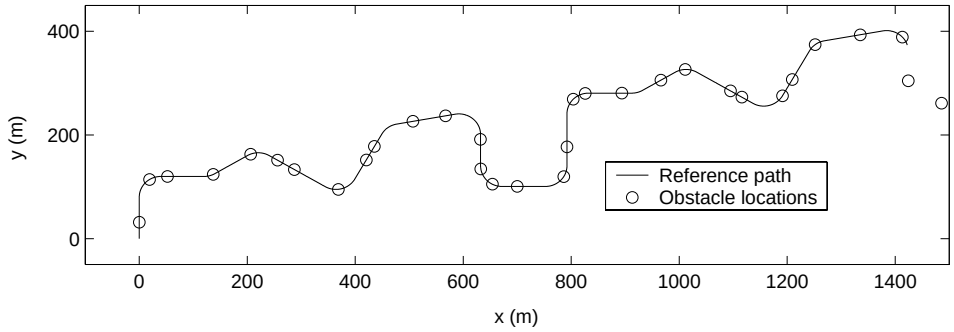

Figure 4. A top-down view of the driving course that subjects travelled during each trial.

accordance with University of Michigan human subject protection policies.

Each subject was asked to use the motorized steering wheel to steer the simulated vehicle along the centerline of the roadway as closely as possible without colliding with any obstacles. Each subject spent one five-minute trial familiarizing him or herself with the path following task under the various experimental conditions. The experimental conditions of concern in Experiment I are with and without haptic assist and with visual feedback occluded except as requested by the driver as described next.

3.2. Measure of Visual Demand

To measure the participants' demand for visual cues, the visual occlusion method was used [9]. The graphical display of the driving environment and roadway were blank except for one-second glimpses provided each time participants pressed a key on the computer keyboard. Subjects were instructed to request the display whenever they felt it necessary to perform the driving task (path following and obstacle avoidance). A measure of visual demand throughout the trial is then provided by the the frequency at which the subject pressed the key.

In all, Experiment I measured three dependent variables across the two conditions, with and without haptic assist. The first two dependent variables were measures of performance on obstacle avoidance and path following. Path following performance was taken as the standard deviation of the perpendicular distance $\overline{CP}$ to the path. Obstacle avoidance performance was determined simply as the number of obstacles successfully avoided, an integer between 0 and 30. The simulator logged the number of obstacle collisions and the vehicle's lateral deviation from the reference path. The last dependent variable was the key press frequency, given by $\frac{\text{\# key presses}}{300s}$.

Performance by each subject on the primary task was recorded under the imposed conditions of the the visual occlusion method for two 5-minute trials: one trial without the haptic assist and the other trial with the haptic assist.

3.3. Results

Figure 6 shows the tracking performance of a typical subject in a generic section of the roadway with and without steering assist. The section of roadway shown took 1 minute to traverse at the constant 7 m/s vehicle speed and is slightly less than 420 meters in length, depending on the particular path of the vehicle taken. The top trace shows the curvature of the road, indicating that both right and left turns and straight segments are represented in this section of roadway. Deviation from the centerline is graphed versus time in the lower two traces, where the upper trace (A) was recorded without assist and the lower trace (B) was recorded with steering assist. The '*' symbols indicate the center of obstacles. A collision occurs if the vehicle center comes within 1.6 meters of an obstacle center. Obstacle avoidance maneuvers produced by the driver are apparent in both traces, and those maneuvers are not appreciably different by condition. Differences across condition are apparent, however, in the tracking performance in the sections of roadway between obstacles. Improvement can be observed in trace (B), where steering assist was provided. To facilitate analysis of lane keeping behavior and its dependence on assist condition independent of the obstacle avoidance maneuvers, the data was partitioned into segments between obstacles, and partitioning was defined in time, where 2 seconds of data before and 1 second after the instant at which the closest point on the centerline passed the obstacle was omitted from the analysis. The shaded areas in figure 6 indicate data within that 3 second window.

The statistics of the performance metrics are provided in Table 1. ANOVA shows that subject and assist are primary factors in all of the performance metrics and the interaction of the two factors is weak. To mitigate the influence of inter-subject variability, paired t-tests are applied to the data to determine the statistical significance of the difference in means $\Delta\bar{x}$. The lateral deviation metric and the visual demand metric clearly show statistical significance, so the 34% reduction in lateral deviation and the 29% reduction in visual demand due to the presence of haptic as-

Measurement	No Assist		With Assist			
	$\bar{x}$	s	$\bar{x}$	s	$\Delta\bar{x}$	p-value
STD[$e(t)$] (m)	1.015	0.462	0.673	0.271	-0.343	0.0028
Obstacles Hit (%)	1.70	2.92	5.97	8.20	+4.26	0.0456
Visual Demand (request/s)	0.570	0.0966	0.404	0.0765	-0.166	< 0.0001

Table 1. Table of performance measures for Experiment I includes the standard deviation of the lateral error, the percent of obstacles hit and the visual demand as the three metrics.

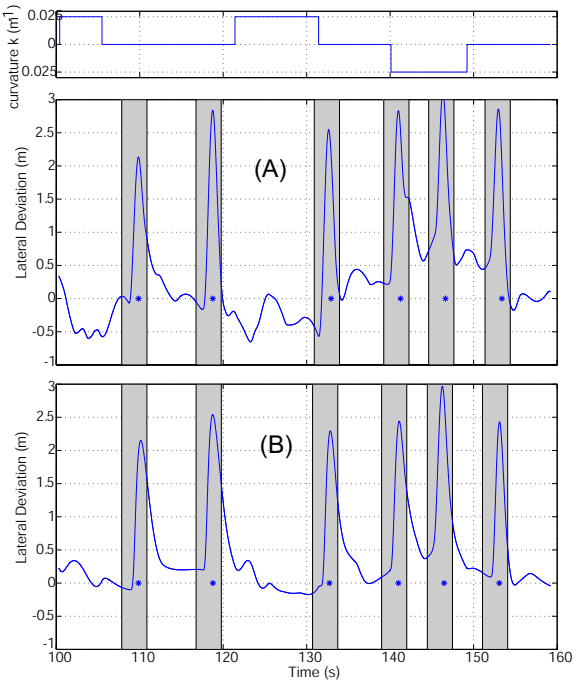

Figure 6. Plot of one subject's lateral deviation for a 1 minute section of roadway under conditions (A) without steering assist and (B) with steering assist. The top trace indicates roadway curvature while * symbols indicate the location of obstacles.

sist can be asserted with a high degree of confidence.

With assist, the percentage of obstacles hit by subjects increases from 1.7% to 6.0%. This is both a statistically significant and important result, however it is not a surprising result. The assist is always trying to drive the vehicle back to the center of the road and that is exactly where the obstacles are placed. Without human intervention, the car would drive through every obstacle on the course. There is a trade-off made in using a control system: by reducing the risk of lane departure, the risk of hitting objects in the lane is increased. See the discussion section for methods to ameliorate the increased risk of in-lane collisions with obstacles.

4. Experiment II

4.1. Protocol

The second experiment was aimed at quantifying the ability of the haptic assist steering wheel to aid the subject in a path following task while reducing the load on his processing capacity.

4.2. Secondary Task: Tone Location

The primary task was the same as in Experiment I: to follow the center of the road as closely as possible but to avoid obstacles. Experiment II, however, included a secondary task designed to require some of the same cognitive processing resources as the primary task, in particular spatial reasoning [10].

Three computer speakers were placed approximately 1 m in front of the driver's head and 18 cm from one another on top of the computer monitor that displayed the roadway. These speakers played half-second square-wave tones with a fundamental frequency of middle-C. The sound-level reading at the subjects head location was measured to be 81 dBA. The time between tones was randomly selected with a uniform distribution between 2 and 6 seconds. Subjects were asked to identify which of the three speakers played the tone and press a corresponding key on the computer keyboard. The key 'j' was used by the subject to indicate that the left speaker had played, the 'k' key the center speaker, and the 'l' key the right speaker.

Two performance metrics were defined for the secondary tone location task: accuracy, or proper identification of the speaker that sounded and the time required to respond, or the reaction time. The accuracy was defined as the percentage of tones that were correctly identified. The response time was the time, in milliseconds, between the tone onset and the registration of the key press by the personal computer. Because of technical limitations, the response times were quantized to 8 millisecond levels. The precision of the timing, however, was better than 1 microsecond. Quantization and jitter in the software can be considered noise.

Performance by each subject on both the primary and secondary tasks was recorded for two 5-minute trials: one trial without the haptic assist and the other trial with the haptic assist.

Measurement	No Assist		With Assist			
	$\bar{x}$	s	$\bar{x}$	s	$\Delta\bar{x}$	p-value
STD[$e(t)$] (m)	0.623	0.385	0.372	0.160	-0.251	0.0071
Obstacles Hit (%)	3.41	6.47	4.26	5.46	+0.85	0.287
Location Accuracy (%)	94.91	4.41	95.26	3.92	+0.35	0.604
Reaction Time (ms)	564	163	545	149	-18.2	0.000903

Table 2. Table of performance metrics for Experiment II includes the standard deviation of the lateral error, the percent of obstacles hit, the percent of tones correctly localized and the reaction-time in locating the tones.

4.3. Results

The means and standard deviations of the performance metrics are given in Table 2. The primary task performance metrics are the lateral deviation performance and the obstacle avoidance performance. Lane-keeping is clearly improved with the addition of haptic assist, but the increase in the percent of obstacles hit was not statistically significant (p=0.287) as it was during Experiement I (p=0.0456). There may however still be an underlying deterioration in the obstacle avoidance as suggested by the data in Experiment I, and the discussion section for possible methods of addressing the problem.

When subjects performed the tone location experiment, their responses were recorded as correct or incorrect and a reaction time (i.e. the time between the beginning of the tone and the keyboard response) was calculated. Both of these values were used to measure the performance of the subject in the secondary task, however the subjects were not told that their performance would be measured by the speed of their response.

The accuracy of the tone location performance is defined as the percentage of correct responses. Comparisons of this performance variable were made across tone location experiments of the same subject for the same speaker location, with and without assist. The difference in the mean percentage of correct responses rose slightly in the trials with haptic assist, however, this result is not statistically significant (p=0.604).

The mean reaction time was the other performance metric for the secondary task. The difference in the mean reaction time with haptic assist and without assist was found by first applying a transformation to the RT (reaction time) data. Several data transformations, including 1/RT, Log(RT) and truncations of the RT data at 0.7, 1.0, 1.25, 1.5 and 2.0 seconds, were applied to the data. By comparing the data with the work on reaction time data by Ratcliff, it was determined that it was appropriate to truncate the data at 1.25 seconds and that the difference in means is primarily in the tail of the data [11]. A statistically significant 18 ms decrease of the reaction time was found with haptic assist compared to no assist (p=0.0009). Despite quantization of timing data, the high precision of the timing data and low software jitter allows the mean difference to be extracted with similar precision (+-0.5ms).

5. Discussion

The same 11 subjects that participated in Experiment I also participated in Experiment II. Trials (5-minute runs on the driving course) pertinent to Experiment II were randomized among the trials for Experiment I. Additionally, two baseline trials were run by each subject; one trial without assist and one trial with assist. The baseline trials were used assess the performance metrics in the absence of any secondary task or visual occlusion. The performance statistics from the baseline trials are in Table 3.

5.1. Visual Demand

The data suggest that when using a haptic assist steering wheel rather than a traditional passive steering wheel, subjects are better able to follow a reference path and at the same time, they required fewer visual cues. Statistical t-tests performed on the mean lateral reference path deviation and visual demand metrics verified the significance of the difference in means between the two groups (with haptic feedback/without haptic feedback). Although subjects found the driving task less visually demanding and had better lane-keeping performance with haptic assist, they also hit more obstacles, which is a clear cost of haptic assist.

The natural consequence of a system that helps prevent lane-departure is an increased probability of in-lane collisions, however this is not an argument against haptic assist. Instead it is a motivation for collision warning and collision avoidance systems that can reduce the chance of an in-lane obstacle collision. A collision warning system would alert the driver through aural, visual or haptic feedback of a possible collision. A slightly more proactive system would disengage the haptic assist along with providing a warning when it sensed an imminent collision. A very sophisticated control system would assess the traffic situation and help the driver make an evasive maneuver.

Measurement	No Assist		With Assist			
	$\bar{x}$	s	$\bar{x}$	s	$\Delta\bar{x}$	p-value
STD[$e(t)$] (m)	0.521	0.319	0.356	0.184	-0.164	0.0255
Obstacles Hit (%)	0.57	1.26	2.84	2.95	+2.27	0.00594

Table 3. Table of performance metrics for the baseline trials includes the standard deviation of the lateral error and the percent of obstacles hit measured with and without assist.

5.2. Tone Location Performance

Accuracy and reaction time were the metrics of subjects' performance in the tone location experiment. The hypothesis of experiment II was that the performance of the secondary task would improve if the driver was provided haptic assist. Indeed, there was an improvement (reduction) of the reaction time by 18ms (p=0.0009), but the improvement in the accuracy was small and not statistically significant. The reduction in reaction time is interesting because it is a desirable result by itself, and it can also be viewed as an indication that the haptic assist increases the available of cognitive processing capacity for the performance of a secondary task.

The presence of the secondary task decreased the lane-keeping performance by 20%, when compared with the baseline experiment with no assist. This statistic is evidence that the spatial reasoning task selected for the secondary task is competing for some of the same cognitive processing capacity required for driving (the primary task). When haptic assist is enabled and the lane-keeping performance of the baseline is compared with the lane-keeping in the presence of the secondary task, there is only a 4% degradation in the lane-keeping. This result suggests that the haptic assist can allow a driver to perform a secondary task with negligible degradation in tracking performance.

6. Summary

We have investigated the use of haptic interface to realize and test the idea of a human driver sharing control of vehicle heading with an automatic controller. The human and controller share the same control interface (e.g. steering wheel) and are mechanically interconnected such that they may exchange not just information with one another but also energy. Haptic display becomes the means to place the automatic controller in the haptic perceptual space of the human. The human is free to monitor the actions of the controller but may over-ride them at any time he sees fit, based on his perception of additional performance factors in the task environment. Shared control extends the notion of a virtual fixture to a virtual agent or co-pilot. Like the virtual fixture, the human is aware of the virtual agent by feel and he can use the agent to more efficiently negotiate a task.

We have completed a human subject experiment that tests a hypothesis involving shared control, that mental workload will be reduced and resources made available for secondary, simultaneous tasks. In a path following task for land vehicles, we see significantly less visual demand and improved performance in both the primary driving task and a secondary task with the aid of a haptic steering wheel.

References

[1] T. B. Sheridan, "Human centered automation: Oxymoron or common sense?," pp. 823–828, IEEE, 1995.

[2] L. Rosenberg, "Virtual haptic overlays enhance performance in telepresence tasks," in *Telemanipulator and Telepresence Technologies*, vol. 2351, pp. 99–108, 1994.

[3] M. Li and A. M. Okamura, "Recognition of operator motions for real-time assistance using virtual fixtures," in *11th International Symposium on Haptic Interfaces for Virtual Environment and Teleoperator Systems, IEEE Virtual Reality*, pp. 125–31, 2003.

[4] T. Bell, "Automatic tractor guidance using carrier-phase differential GPS," *Computers and Electronics in Agriculture*, vol. 25, pp. 53–66, 2000.

[5] M. Steele and R. B. Gillespie, "Shared control between human and machine: Using a haptic interface to aid in land vehicle guidance," in *Proceedings of the Human Factors and Ergonomics Society 45th Annual Meeting*, pp. 1671–1675, 2001.

[6] K. Suzuki and H. Jansson, "An analysis of driver's steering behaviour during auditory or haptic warnings for the designing of lane departure warning system," *JSAE Review*, vol. 24, pp. 65–70, January 2003.

[7] J. Schumann, J. Godthelp, and W. Hoekstra, "An exploratory simulator study on the use of active control devices in car driving," Tech. Rep. Report No. IZF 1992 B-2, Soesterberg, Netherlands. Institute for Perception TNO, 1992.

[8] R. A. Hess and A. Modjtahedzadeh, "A control theoretic model of driver steering behavior," *IEEE Control Systems Magazine*, pp. 3–8, August 1990.

[9] P. Green, "Visual and task demands of driver information systems," Tech. Rep. Tech Report UMTRI-98-16, University of Michigan Research Institute., 1998.

[10] C. D. Wickens and L. Liu, "Codes and modalities in multiple resources: a success and a qualification," *Human Factors*, vol. 30, no. 5, pp. 599–616, 1988.

[11] R. Ratcliff, "Methods for dealing with reaction time outliers," *Psychological Bulletin*, vol. 114, no. 3, pp. 510–32, 1993.